

The role of tetragonal side morphotropic phase boundary in modified relaxor-PbTiO₃ crystals for high power transducer applications

Lingping Kong, Gang Liu, Shujun Zhang, and Haozhe Liu

Citation: *J. Appl. Phys.* **114**, 144106 (2013); doi: 10.1063/1.4824185

View online: <http://dx.doi.org/10.1063/1.4824185>

View Table of Contents: <http://jap.aip.org/resource/1/JAPIAU/v114/i14>

Published by the AIP Publishing LLC.

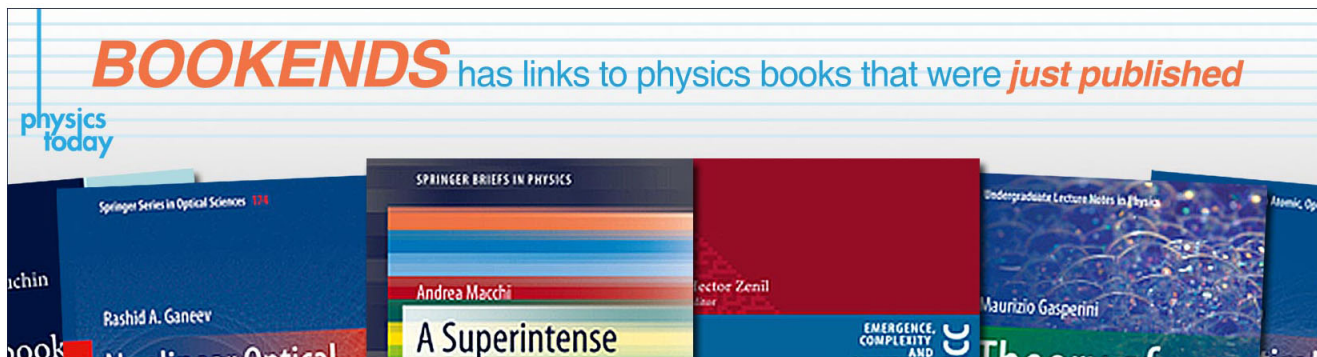
Additional information on J. Appl. Phys.

Journal Homepage: <http://jap.aip.org/>

Journal Information: http://jap.aip.org/about/about_the_journal

Top downloads: http://jap.aip.org/features/most_downloaded

Information for Authors: <http://jap.aip.org/authors>



The role of tetragonal side morphotropic phase boundary in modified relaxor-PbTiO₃ crystals for high power transducer applications

Lingping Kong,^{1,2,3} Gang Liu,^{1,2,4,a)} Shujun Zhang,^{4,a)} and Haozhe Liu¹

¹Harbin Institute of Technology, Harbin 150080, People's Republic of China

²Center for High Pressure Science and Technology Advanced Research, 1690 Cailun Road, Pudong, Shanghai 201203, People's Republic of China

³HPSynC, Carnegie Institution of Washington, Argonne, Illinois 60439, USA

⁴Materials Research Institute, The Pennsylvania State University, University Park, Pennsylvania 16802, USA

(Received 14 September 2013; accepted 17 September 2013; published online 11 October 2013)

Morphotropic phase boundary (MPB) in ferroelectric materials leads to improved properties due to the structural instability. The manganese modified Pb(In_{1/2}Nb_{1/2})O₃-Pb(Mg_{1/3}Nb_{2/3})O₃-PbTiO₃ crystals with MPB composition were investigated, the structure/property relationship was established. The tetragonal side MPB (coexistence of 91% tetragonal and 9% monoclinic phases) was confirmed by X-ray synchrotron data, while relaxor behavior was detected by Raman characterization and dielectric measurement. Crystals with such MPB composition possess high “figure of merit” ($d_{33} \cdot Q_{33} \sim 10^6$ pC/N), being one order higher when compared with their pure rhombohedral counterparts. Together with high Curie temperature (~ 229 °C) and temperature stability of properties, demonstrating a promising candidate for high power transducer applications.

© 2013 AIP Publishing LLC. [<http://dx.doi.org/10.1063/1.4824185>]

I. INTRODUCTION

The morphotropic phase boundary (MPB), which separates two ferroelectric phases with different crystallographic symmetries in the composition-temperature phase diagram of ferroelectric solid solution, can lead to a great enhancement of piezoelectric activity.^{1,2} However, a high energy dissipation (or low mechanical quality factor Q) exists near the MPB region, being associated with the instability of the coexistent phases.³ Relaxor-PbTiO₃ single crystals, such as $(1-x)\text{Pb}(\text{Mg}_{1/3}\text{Nb}_{2/3})\text{O}_3-x\text{PbTiO}_3$ (PMN-PT) and $(1-x-y)\text{Pb}(\text{In}_{1/2}\text{Nb}_{1/2})\text{O}_3-x\text{Pb}(\text{Mg}_{1/3}\text{Nb}_{2/3})\text{O}_3-y\text{PbTiO}_3$ (PIN-PMN-PT), have been the mainstay of ferroelectric material studies in last 20 years, promising for next generation electromechanical applications.³⁻⁵ Rhombohedral PMN-PT crystals poled along the nonpolar $[001]_c$ direction were reported to possess high electromechanical coupling factors $k_{33} > 0.9$ and large piezoelectric coefficients $d_{33} > 1500$ pC/N.^{3,4} Nevertheless, their usage for high power transducers has been limited by the low ferroelectric phase transition temperature and mechanical quality factor Q , being on the order of 130 °C and 100, respectively.³ Utilizing crystals with tetragonal phase is expected to broaden the usage temperature range greatly, due to the fact that there is no ferroelectric phase transition occurring above room temperature and prior to their Curie temperatures. For example, the $[001]_c$ poled tetragonal PIN-PMN-PT crystals were reported to possess high T_c , being on the order of 220 °C, with a relatively high electromechanical coupling $k_{33} \sim 0.84$, which maintains similar value up to 200 °C.⁶ On the other hand, the acceptor doped relaxor-PT crystals with engineered domain configurations, such as manganese (Mn) modified $\text{Pb}(\text{Mg}_{1/3}\text{Nb}_{2/3})\text{O}_3\text{-PbZrO}_3\text{-PbTiO}_3$ (PMN-PZT) and PIN-PMN-PT crystals,^{7,8} were reported to possess significantly

improved quality factors or decreased dissipation factors, which can be understood by the domain wall clamping/polarization rotation restriction effect associated with the internal bias, which is induced by the acceptor-oxygen vacancy defect dipoles.³ Thus, it is important to study microstructure and macroscopic properties of the acceptor modified tetragonal relaxor-PT crystals, which are expected to offer wide usage temperature range, high temperature stability of piezoelectric activity, and low energy dissipation. In the present work, the temperature dependence of crystal structure, phase transition, and electromechanical properties of manganese modified tetragonal PIN-PMN-PT crystals were investigated, with emphasis on the importance of the monoclinic/tetragonal MPB.

II. EXPERIMENTAL

The Mn modified PIN-PMN-PT crystals (referred to as “PIN-PMN-PT:Mn” in the present work) were grown using modified Bridgman method.⁹ The studied composition, 0.26PIN-0.39PMN-0.35PT, was selected on the tetragonal side of the monoclinic/tetragonal MPB composition. The ultrafine crystal structure was measured up to 300 °C in transmission geometry, using high-resolution synchrotron X-ray diffraction (XRD) on beamline 11-BM (Advanced Photon Source at Argonne National Laboratory). Using a scintillator based multichannel analyzer detector at 11-BM, the resolution is $\Delta Q/Q = 1.7 \times 10^{-4}$, representing the state-of-the-art angular resolution for powder diffraction measurements. Diffraction patterns were measured using an X-ray wavelength of 0.413566 Å over 2θ range of 4.0°–24.0°, with a 0.002° 2θ step-size. Raman spectroscopy measurements up to 400 °C were performed with the 514.5 nm excitation laser. For property characterization, all samples were cut from same crystal wafer and oriented using the real-time Laue X-ray system with an accuracy of $\pm 0.5^\circ$. Each sample was cut and polished with three pairs of parallel

^{a)}Authors to whom correspondence should be addressed. Electronic addresses: hit071202@gmail.com (G. Liu) and soz1@psu.edu (S. J. Zhang)

surfaces along $[001]_c$, $[010]_c$, and $[100]_c$ crystallographic directions. The samples were electroded using sputtered gold thin film and poled under a dc field of 3 kV/cm at 230 °C (above the Curie temperature), subsequently field cooled to room temperature to avoid cracking.¹⁰ Complete set of elastic, dielectric, and piezoelectric constants of $[001]_c$ poled crystals was determined by combined resonance and ultrasonic methods.¹¹ For resonance measurements, the dimensions and geometries of the samples were specified by the IEEE standards on piezoelectricity.¹² The dielectric properties as a function of temperature were measured using HP4284A precision LCR meter connected to a computer controlled temperature chamber. The temperature dependence of the elastic constants, electromechanical coupling factors, and piezoelectric coefficients were measured using HP4194A impedance phase-gain analyzer connected to a temperature chamber.

III. RESULTS AND DISCUSSIONS

To investigate the crystal structure and phase transition sequence, *in-situ* high resolution synchrotron XRD was employed. Figure 1(a) shows Bragg reflections of PIN-PMN-PT:Mn from room temperature to 300 °C. At room temperature, the (111) reflection appears asymmetric, while both (110) and (200) reflections exhibit distinct multi-peak characteristics. Above 230 °C, all three reflections become symmetric, suggesting a cubic $Pm\bar{3}m$ space group. These XRD patterns were modeled using the Rietveld refinement

program GSAS and the results were plotted in Figure 1(b). At room temperature, the obtained XRD pattern cannot be fitted with any single space group model (including monoclinic Cm , tetragonal $P4mm$, or rhombohedral $R3c$), while it can be fitted with the $Cm + P4mm$ mixed phases. This observed coexistence of two phases confirms a tetragonal side of the monoclinic/tetragonal MPB composition. At 213 °C and 231 °C, the XRD patterns can be fitted by tetragonal $P4mm$ and cubic $Pm\bar{3}m$ models, respectively, demonstrating a phase transformation from tetragonal ferroelectric to paraelectric phase occurs in this temperature range. The temperature dependences of the lattice parameters, as well as the fraction of monoclinic phase were given in Figures 1(c) and 1(d), respectively. It was observed that the PIN-PMN-PT:Mn remained mixed phases, with coexistence of monoclinic and tetragonal phases up to approximately 150 °C, then transformed to a single tetragonal phase. Of particular interest is that the β angle increases slightly as a function of temperature, while the fraction of monoclinic phase decreases greatly, implying that there is no continuous polarization rotation with increasing temperature up to tetragonal phase, similar phenomenon was also observed for PMN-PT.¹³ It has been reported that the role of the monoclinic phase is only to form an MPB with rhombohedral or tetragonal phase, while phase (structure) instability is the dominant factor for inducing a high piezoelectric response.^{3,14} Thus, although the fraction of monoclinic Cm phase is very low, being on the order of 9% at room temperature and decreased to 4% at 150 °C, high piezoelectric activity induced by the

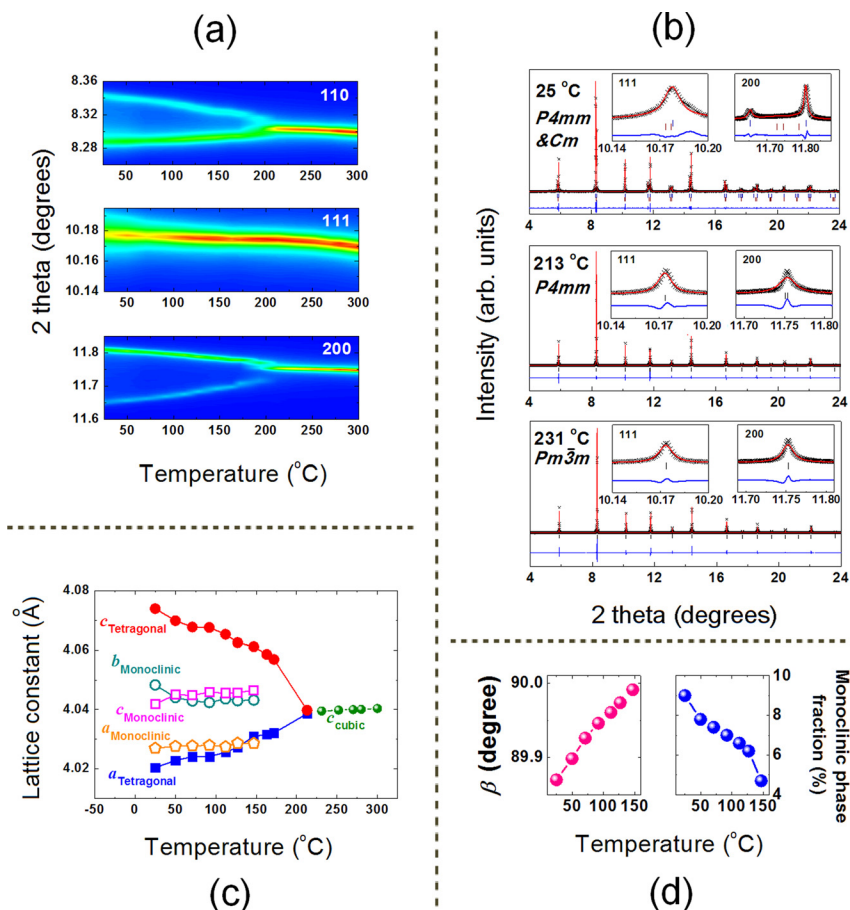


FIG. 1. Synchrotron XRD results on PIN-PMN-PT:Mn crystals: (a) Selected Bragg reflections from room temperature to 300 °C; (b) Rietveld refinement of the patterns measured at 25 °C, 213 °C, 231 °C; (c) temperature dependence of lattice constants; and (d) temperature dependence of β angle and fraction of monoclinic phase.

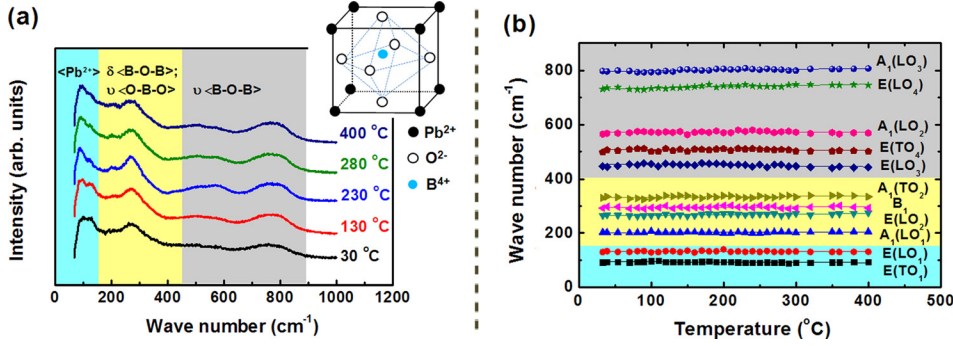


FIG. 2. (a) Temperature-dependent Raman spectra for PIN-PMN-PT:Mn as a function of temperature. (b) Temperature dependence of the Raman bands. The solid lines are the linear fitting results.

phase instability on the proximity of MPB region can be expected.

The relaxor-PT systems, especially those with MPB compositions, were reported to be highly disordered and inhomogeneous.¹⁵ To further understand these materials, investigation on local phenomena should be carried out.¹⁶ Figure 2(a) shows the Raman-scattering spectra measured on PIN-PMN-PT:Mn up to 400 °C. It was observed that all Raman bands are relatively broad, being associated with the band overlapping, demonstrating a typical characteristic of relaxor ferroelectrics. In addition, the Raman spectra measured at 400 °C were found to be similar to those measured at lower temperatures, suggesting that a local disorder feature yet exists above Curie temperature. This is related to the chemical inhomogeneity (Mg, Nb, In, Ti, and Mn) on *B* sites of the perovskite structure, though the average macroscopic crystal structure is paraelectric Cubic. The Raman spectra can be divided into three regions of frequency: the low frequency region (approximately up to 150 cm^{-1}); intermediate frequency region (150–450 cm^{-1}); and high frequency region (450–900 cm^{-1}). Based on the lattice dynamics calculation and mode assignment method for PMN and PMN-PT,^{16–18} the low frequency region is attributed to the

Pb-BO_6 stretching mode ($\langle\text{Pb}^{2+}\rangle$), while the modes in intermediate frequency region can be classified as *B-O-B* bending (δ) and *O-B-O* stretching (ν), and the vibrations occurred in high frequency region are attribute to *B-O-B* stretching. Using a PEAKFIT software program by Jandel Scientific, the corresponding peak positions of the Raman mode as a function of temperature are determined and presented in Figure 2(b). Then, according to the reported data for PMN-PT and PbTiO_3 ,^{19,20} all these modes can be assigned (listed in Figure 2(b)). It was observed that the Raman frequencies maintained the same values as a function of temperature for all vibration modes, revealing a strong temperature stability of the local structure.

When the crystal is poled along $[001]_c$ crystallographic direction, the domain patterns of monoclinic or tetragonal crystals were found to be multi-domain “4O” or single-domain “1T” configuration, respectively, both exhibiting macroscopic $4mm$ symmetry. Based on the XRD results measured at room temperature, “1T” and “4O” domain configurations were found to coexist in the poled crystals, with the fraction of “1T” being on the order of $\sim 91\%$, thus a pseudo-single-domain state is reasonable. Table I lists the complete set of elastic, dielectric, and piezoelectric constants of

TABLE I. Material properties of tetragonal PIN-PMN-PT:Mn single crystals poled along $[001]_c$ crystallographic direction.

Elastic stiffness constants: c^E, c^D (10^{10} N/m ²)											
c_{11}^E	c_{12}^E	c_{13}^E	c_{33}^E	c_{44}^E	c_{66}^E	c_{11}^D	c_{12}^D	c_{13}^D	c_{33}^D	c_{44}^D	c_{66}^D
19.07	13.64	12.20	11.53	2.49	7.50	19.12	13.69	11.73	16.25	7.38	7.50
Elastic compliance constants: s^E, s^D (10^{-12} m ² /N)											
s_{11}^E	s_{12}^E	s_{13}^E	s_{33}^E	s_{44}^E	s_{66}^E	s_{11}^D	s_{12}^D	s_{13}^D	s_{33}^D	s_{44}^D	s_{66}^D
16.48	-1.93	-15.40	41.27	40.16	13.33	12.36	-6.05	-4.56	12.74	13.54	13.33
Piezoelectric constants: d (10^{-12} C/N), e (C/m ²), g (10^{-3} Vm/N), h (10^8 V/m)											
d_{15}	d_{31}	d_{33}	e_{15}	e_{31}	e_{33}	g_{15}	g_{31}	g_{33}	h_{15}	h_{31}	h_{33}
1750	-190	500	43.58	-1.13	11.27	15.21	-21.69	57.07	11.23	-4.18	41.82
Dielectric constants: $\varepsilon(\varepsilon_0), \beta$ ($10^{-4}/\varepsilon_0$)						Density (kg/m ³)					
ε_{11}^S	ε_{33}^S	ε_{11}^T	ε_{33}^T	β_{11}^S	β_{33}^S	β_{11}^T	β_{33}^T	ρ			
4384	305	13000	990	2.28	32.83	0.77	10.10	8150			
Electromechanical coupling factors: k						Mechanical quality factors: Q					
k_{15}	k_{31}	k_{33}	k_t	Q_{15}	Q_{31}	Q_{33}	Q_t				
0.81	0.50	0.83	0.54	150	550	2000	200				

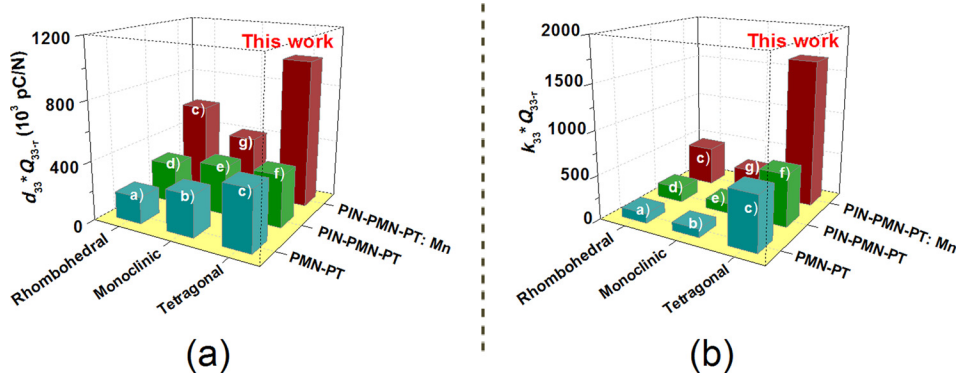


FIG. 3. Comparison of FOM $d \cdot Q$ (a) and $k \cdot Q$ (b) for PMN-PT, PIN-PMN-PT, and PIN-PMN-PT:Mn crystals with various phases. Data of (a)–(g) are from Refs. 3, 5, 21, 29–32, respectively.

[001]_c-poled PIN-PMN-PT:Mn crystals. The shear piezoelectric coefficient d_{15} was found to be on the order of 1750 pC/N, due to the fact that the applied field is perpendicular to the poling direction in the single domain state, thus facilitated “polarization rotation.” However, this value is much smaller when compared with its pure counterpart, ~ 2350 pC/N,⁶ demonstrating that the internal bias in PIN-PMN-PT:Mn restrict the polarization rotation, which can also be confirmed by the high shear mechanical quality factor Q_{15-T} , being on the order of ~ 150 , five times higher than those of pure crystals (< 30).³ On the contrary, the extensional piezoelectric properties of modified PIN-PMN-PT crystals, including the longitudinal d_{33} and lateral d_{31} , were comparable with those of pure tetragonal PIN-PMN-PT, due to the fact that the phase instability inherently associated with MPB contribute to the high piezoelectric activity, while the acceptor dopant (internal bias) has minimal effect on the polarization extension in single domain state.^{3,10,21} Of particular significance is that the mechanical quality factors show very high values, being on the order of 2000 for the longitudinal mode, which can be explained by the following two aspects: on one hand, the absence of domain wall in single domain state “1T” is critical for the low energy dissipation and high mechanical quality factors;²² on the other hand, the acceptor Mn^{2+} , $^{3+}$ dopants in the monoclinic “4O” domain state clamp domain wall motion and restrict polarization rotations, accounting for the enhanced Q values.⁷

For high power transducer applications, such as underwater acoustic transducers and high intensity focused ultrasound, high electromechanical coupling k and/or large piezoelectric coefficient d allows for increased transducer bandwidth and sensitivity, while high mechanical quality factor Q reduces heat generation and increases acoustic power output under high drive conditions, thus the figure of merit (FOM) of the materials is defined as the product of k and Q (or the product of d and Q).^{23–25} Figure 3 gives the FOM ($k \cdot Q$ or $d \cdot Q$ value) of the studied PIN-PMN-PT:Mn crystals, which were found to be 2–10 times higher than those of unmodified PMN-PT, PIN-PMN-PT crystals, and Mn modified rhombohedral PIN-PMN-PT crystals. This high figure of merit makes tetragonal PIN-PMN-PT:Mn promising materials for next generation high power transducers.

It is generally accepted that temperature stability of properties is important for practical applications, due to the fact that most electromechanical devices require operation in

a variable temperature ranges.³ To investigate the temperature stability for [001]_c poled PIN-PMN-PT:Mn crystals, the dielectric and electromechanical properties have been evaluated as a function of temperature. Figure 4 shows the dielectric behavior as a function of temperature for [001]_c poled PIN-PMN-PT:Mn crystals. The Curie temperature T_c was found to be on the order of 229 °C, 50 °C higher than those of tetragonal PMN-PT,²⁶ in good agreement with that determined by high temperature XRD patterns. The relaxor behavior of ferroelectric crystals can be described by a modified Curie law given in the following equation:

$$\frac{1}{\varepsilon} - \frac{1}{\varepsilon_m} = \frac{(T - T_m)^\gamma}{C}, \quad (1)$$

where ε_m is the maximum value of the dielectric permittivity at T_m , C is the Curie-like constant, and γ is the degree of diffuseness. The experimental data shown in Figure 4 can be well fitted to Eq. (1), with a γ value being on the order of 1.65 (see the inset of Figure 4). This value is much higher than those of tetragonal PMN-PT crystals (< 1.3),² suggesting that a relaxor-like behavior cannot be ignored in PIN-PMN-PT crystals with monoclinic/tetragonal MPB composition, which can be confirmed by the Raman spectra (Figure 2(a)). The relaxor characteristic of tetragonal PIN-PMN-PT crystals also contributes to the high piezoelectric activity when compared with their binary counterparts (~ 500 pC/N vs < 300 pC/N).^{3,27,28}

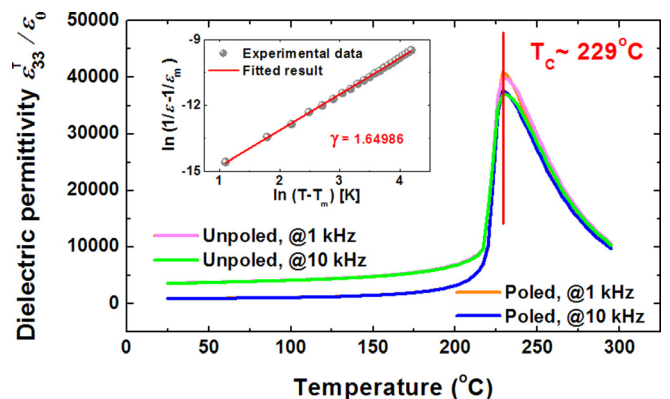


FIG. 4. Temperature dependence of dielectric permittivity $\varepsilon_{33}^T/\varepsilon_0$ (measured at 1 kHz and 10 kHz) for [001]_c poled PIN-PMN-PT:Mn crystals, small inset is the dielectric permittivity vs. temperature relationship.

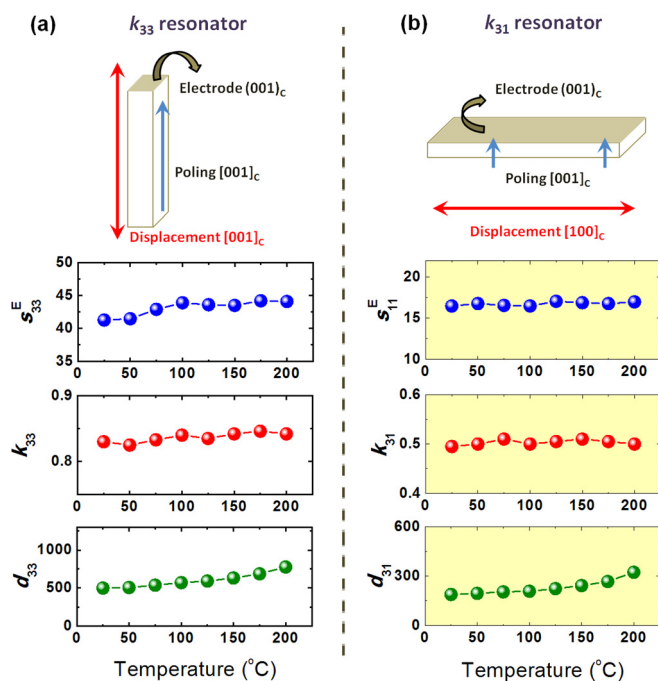


FIG. 5. Temperature dependence of electromechanical coupling factor, elastic, and piezoelectric coefficients for PIN-PMN-PT:Mn crystals: (a) longitudinal k_{33} -mode and (b) lateral k_{31} -mode.

Figure 5 gives the temperature dependence of the elastic, electromechanical, and piezoelectric properties as a function of temperature for longitudinal k_{33} - (a) and lateral k_{31} -mode (b). For both k_{33} - and k_{31} -resonators, nearly temperature-independent elastic constants and electromechanical coupling factors were observed. In addition, the piezoelectric coefficients d_{33} and d_{31} were found to increase slightly, being 25% and 18% in the temperature range of 25 °C to 150 °C, respectively. Thus, high temperature stability of properties can be confirmed, which was thought to be associated with the absence of ferroelectric phase transition above room temperature and the high Curie temperature, being on the order of 229 °C.

IV. CONCLUSION

In conclusion, a tetragonal side MPB was observed in manganese modified ternary PIN-PMN-PT crystals, separating monoclinic and tetragonal ferroelectric phases. Using high-resolution synchrotron XRD, a coexistence of monoclinic and tetragonal phases was confirmed. Such a tetragonal-side MPB leads to (1) high piezoelectric activity ($d_{33} \sim 500$ pC/N) due to the phase (structure) instability and relaxor characteristic; (2) low energy dissipation ($Q_{33} \sim 2000$) being attribute to the pseudo-single-domain state and restriction of polarization rotation; and (3) high temperature stability of properties associated with the high Curie temperature (~ 229 °C) of tetragonal crystals. Here, (1) and (2) cooperatively contribute to a superior FOM, together with (3), make these materials potential for high power transducer applications. In addition, the results on tetragonal side MPB provide an alternative approach for developing high-performance

ferroelectric materials, and shed some lights on understanding the complicated MPB in other ferroic systems.

ACKNOWLEDGMENTS

The authors specially thank Dr. Matthew R. Suchomel for experimental help and useful discussions. Lingping Kong and Gang Liu would like to acknowledge the support from the National Scholarship Council of China. Use of the Advanced Photon Source was supported by the U. S. Department of Energy, Office of Science, Office of Basic Energy Sciences, under Contract No. DE-AC02-06CH11357.

- ¹B. Jaffe, R. S. Roth, and S. Marzullo, *J. Appl. Phys.* **25**, 809 (1954).
- ²D. Damjanovic, *Rep. Prog. Phys.* **61**, 1267 (1998).
- ³S. J. Zhang and F. Li, *J. Appl. Phys.* **111**, 031301 (2012).
- ⁴S. E. Park and T. R. Shrout, *J. Appl. Phys.* **82**, 1804 (1997).
- ⁵S. J. Zhang, J. Luo, W. Hackenberger, and T. R. Shrout, *J. Appl. Phys.* **104**, 064106 (2008).
- ⁶F. Li, S. J. Zhang, Z. Xu, X. Y. Wei, J. Luo, and T. R. Shrout, *J. Appl. Phys.* **107**, 054107 (2010).
- ⁷S. J. Zhang, S. Lee, D. Kim, H. Lee, and T. R. Shrout, *Appl. Phys. Lett.* **93**, 122908 (2008).
- ⁸X. Q. Huo, S. J. Zhang, G. Liu, R. Zhang, J. Luo, R. Sahul, W. W. Cao, and T. R. Shrout, *J. Appl. Phys.* **113**, 074106 (2013).
- ⁹J. Luo, S. J. Zhang, W. Hackenberger, and T. R. Shrout, "Bridgman growth and characterization of relaxor-PT piezoelectric crystals," in Proceedings of the US Navy Workshop on Acoustic Transduction Materials and Devices, State College, PA, 11–13 May 2010.
- ¹⁰F. Li, S. J. Zhang, Z. Xu, X. Y. Wei, and T. R. Shrout, *Adv. Funct. Mater.* **21**, 2118 (2011).
- ¹¹R. Zhang, B. Jiang, and W. Cao, *Appl. Phys. Lett.* **82**, 787 (2003).
- ¹²IEEE Standard on Piezoelectricity (ANSI/IEEE Standard, New York, 1987), p. 176.
- ¹³B. Noheda, D. E. Cox, G. Shirane, J. Gao, and Z.-G. Ye, *Phys. Rev. B* **66**, 054104 (2002).
- ¹⁴F. Li, S. J. Zhang, Z. Xu, X. Y. Wei, J. Luo, and T. R. Shrout, *J. Appl. Phys.* **108**, 034106 (2010).
- ¹⁵D. Viehland, S. J. Jang, L. E. Cross, and M. Wuttig, *J. Appl. Phys.* **68**, 2916 (1990).
- ¹⁶A. Słodczyk, P. Daniel, and A. Kania, *Phys. Rev. B* **77**, 184114 (2008).
- ¹⁷E. Husson, L. Abello, and A. Morell, *Mater. Res. Bull.* **25**, 539 (1990).
- ¹⁸S. A. Prosandeev, E. Cockayne, P. B. Burton, S. Kamba, J. Petzelt, Yu. Yuzuyk, R. S. Katiyar, and S. B. Vakhshuev, *Phys. Rev. B* **70**, 134110 (2004).
- ¹⁹J. D. Freire and R. S. Katiyar, *Phys. Rev. B* **37**, 2074 (1988).
- ²⁰J. A. Lima, W. Paraguassu, P. T. C. Freire, A. G. Souza Filho, C. W. A. Paschoal, J. Mendes Filho, A. L. Zanin, M. H. Lente, D. Garcia, and J. A. Eiras, *J. Raman Spectrosc.* **40**, 1144 (2009).
- ²¹X. Q. Huo, S. J. Zhang, G. Liu, R. Zhang, J. Luo, R. Sahul, W. W. Cao, and T. R. Shrout, *J. Appl. Phys.* **112**, 124113 (2012).
- ²²S. J. Zhang, N. P. Sherlock, R. J. Meyer, and T. R. Shrout, *Appl. Phys. Lett.* **94**, 162906 (2009).
- ²³R. Woollett, *IEEE Trans. Sonics Ultrason.* **15**, 218 (1968).
- ²⁴C. H. Sherman and J. L. Butler, *Transducers and Arrays for Underwater Sound* (Office of Naval Research, 2007), Vol. 124.
- ²⁵S. J. Zhang, R. Xia, L. Lebrun, D. Anderson, and T. Shrout, *Mater. Lett.* **59**, 3471 (2005).
- ²⁶H. Cao, B. Fang, H. Xu, and H. Luo, *Mater. Res. Bull.* **37**, 2135 (2002).
- ²⁷G. Y. Xu, J. S. Wen, C. Stock, and P. M. Gehring, *Nature Mater.* **7**, 562 (2008).
- ²⁸G. Y. Xu, *J. Phys. Soc. Jpn.* **79**, 011011 (2010).
- ²⁹S. Zhang, S. Lee, D. Kim, H. Lee, and T. R. Shrout, *J. Am. Ceram. Soc.* **91**, 683 (2008).
- ³⁰W. Cao, in *Handbook of Advanced Dielectric, Piezoelectric and Ferroelectric Materials—Synthesis, Characterization and Applications*, edited by Z. G. Ye (Woodhead, Cambridge, England, 2008), pp. 235–265.
- ³¹G. Liu, S. J. Zhang, W. H. Jiang, and W. W. Cao, "Energy dissipation in relaxor-PT single crystals: polarization rotation/elongation and domain wall motions," (unpublished).
- ³²D. B. Lin, S. J. Zhang, Z. R. Li, F. Li, Z. Xu, S. Wada, J. Luo, and T. R. Shrout, *J. Appl. Phys.* **110**, 084110 (2011).